Renewable Energy 202 (2023) 442–452

Contents lists available at ScienceDirect

Renewable Energy

journal homepage: www.elsevier.com/locate/renene

Investigating scalability of deep borehole heat exchangers: Numerical modelling of arrays with varied modes of operation

Christopher S. Brown *, Isa Kolo, Gioia Falcone, David Banks

James Watt School of Engineering, University of Glasgow, Glasgow, G12 8QQ, UK

ARTICLE INFO

Keywords:
OpenGeoSys
Deep borehole heat exchanger array
Newcastle science central deep geothermal borehole
Numerical modelling

ABSTRACT

Deep Borehole Heat Exchangers (DBHEs) are a potentially important method of developing geothermal resources through closed-loop systems for carbon neutral, spatial heating. Past research has primarily focused on single-well systems, with few investigating arrays of multiple DBHEs as a method of extracting more thermal energy. In this study, a series of arrays were modelled using OpenGeoSys software, with the aim of understanding the influence of array geometry, inter-borehole spacing and the mode of operation on the thermal performance and system efficiency. OpenGeoSys software is a finite-element model which solves thermal fluxes through the wellbore and surrounding rock using the dual-continuum method. Simulations were undertaken for the lifetime of an array (20 years) with modes of operation testing 1) long-term constant heat load application and 2) intermittent operation with 6 months of extraction followed by a recovery period. Results indicate geometry and mode of operation had a significant impact on inter-borehole spacing and system performance. For long term constant heat load application of 50 kW per DBHE, the minimal spacing required for line and square arrays should be 40 and 30 m. When considering intermittent operation, recovery periods allow replenishment of heat around the borehole, meaning smaller spacing can be utilised.

1. Introduction

Internationally, there is a drive to reduce carbon emissions and limit global warming by transitioning to renewable energy sources. Space heating is traditionally sourced by non-renewable, fossil fuels (typically gas) and represents a significant area for decarbonisation. Whilst a range of renewable energy sources can be developed, geothermal energy has strong potential due to its ability to provide a weather independent, constant base load of energy. Shallow borehole heat exchangers can be coupled to ground sourced heat pumps to extract heat. Typically, these deploy arrays with a u-tube configuration in shallow depths <300 m (e.g. Refs. [1–3]), which is also defined as the regulatory boundary for the UK between shallow and deep geothermal resources by the Infrastructure Act [4]. Increased investigation is, however, occurring in DBHEs, but this is usually focused on single borehole systems (e.g., Refs. [5–9]).

Shallow and deep borehole heat exchangers are affected by local geological, operational and engineering conditions such as thermal conductivity of cement, casing and rock, groundwater flow, flow rate etc., [8,10–13]. The spacing and geometry of the borehole heat exchanger array can also have a significant impact with spacing ideally set to >20 m in shallow settings to reduce thermal interference [14]. Similarly, in deep settings the thermal propagation of the cold front around a DBHE has been shown to be < 15 m over a heating season [8] and <80 m for a 25 year period of operation [15], whilst the limited studies conducted on DBHE arrays have suggested borehole spacing should be over 15 m [16,17]. Therefore, for a DBHE operating to extract heat only, without re-injecting, it is preferred, from the point of view of thermal interference, for the spacing of the array to be as large as possible. In reality, this preference will be balanced against the costs of land, lengths and inefficiencies of header pipework. In this study, simulations were undertaken to test the impact of spacing around the DBHEs, the influence of different methods of operation on DBHE spacing (i.e., intermittent v constant base load extraction) and whether the shape or design of the array has an impact on the performance.

The case study is based upon the real case of the Newcastle Science Central Deep Geothermal Borehole (NSCDGB). This was chosen due to: 1) the high heat flows observed in the area [18,19] which are associated to the geothermal resource concentrated within the North Pennine Batholith [20], 2) currently, there is an ex-geothermal exploration borehole for which a plan is in place to test as a potential DBHE [21], 3)

* Corresponding author.
E-mail address: christopher.brown@glasgow.ac.uk (C.S. Brown).

https://doi.org/10.1016/j.renene.2022.11.100
Received 7 September 2022; Received in revised form 19 November 2022; Accepted 22 November 2022
Available online 23 November 2022

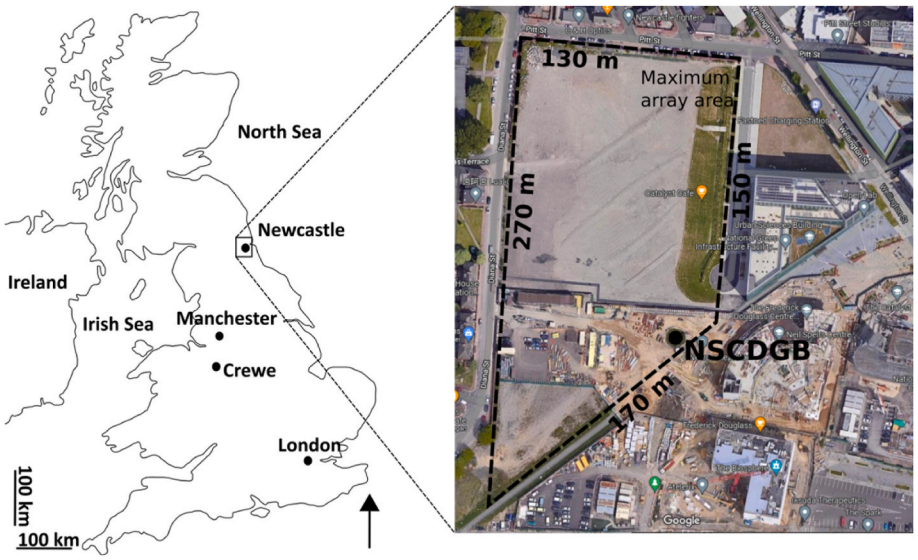

Fig. 1. Map of the UK highlighting Newcastle and the area available for the DBHE array. Satellite image from Google Maps [24].

there is a large amount of land that is available for drilling and 4) estimates of a single DBHE heat extraction rate over a heating season [22] suggest the resource would be unlikely to supply the building demands [23], therefore there is a theoretical opportunity for a DBHE array to be scaled. The geology consists of a Carboniferous succession of sedimentary rocks, with 1821 m penetrated by the NSCDGB [18]. In this case study, the DBHE is limited to 920 m depth as a 4.5 inch (11.43 cm) liner inserted below this depth restricts access for pipework of an acceptable hydraulic performance. The array of DBHEs were therefore, designed with identical parameters to the NSCDGB where there is data on well completion, design, geology and thermal parameters.

In this paper, the model was developed on OpenGeoSys software (e.g., [13,42]) to understand the subsurface response to operation of a DBHE array for the Newcastle Helix area and adjacent buildings (Fig. 1). Long term simulations were carried out to understand the influence of borehole operation, spacing and array layout. Previous analysis on DBHE arrays has focused on a specific case study [16] and array design [17] without testing the impact of different modes of operation. Similarly, minimal research has been undertaken on the mode of operation of single DBHEs, but those who have, suggest that greater mean extraction rates over the period of operation can be supported with longer periods of recovery from horizontal DBHEs (e.g., Ref. [25]). The method of operation has not been extended to DBHE arrays. This study therefore, tests the influence of modes of operation on different array designs and spacing; specifically focusing on constant heat load operation, before comparing it with intermittent operation with periods of rest.

2. Methods

2.1. Numerical modelling approach

OpenGeoSys (OGS) software was utilised to model the performance of the DBHE array in the Newcastle Helix area. The finite element model utilises a 'dual-continuum' approach which treats the DBHE as a 1D discretised medium and the surrounding rock in 3D. In this study, the model uses a CXA (coaxial DBHE) configuration (Fig. 2). Fluid is circulated down the annular space before being circulated to the surface through the central pipe. The models developed only consider

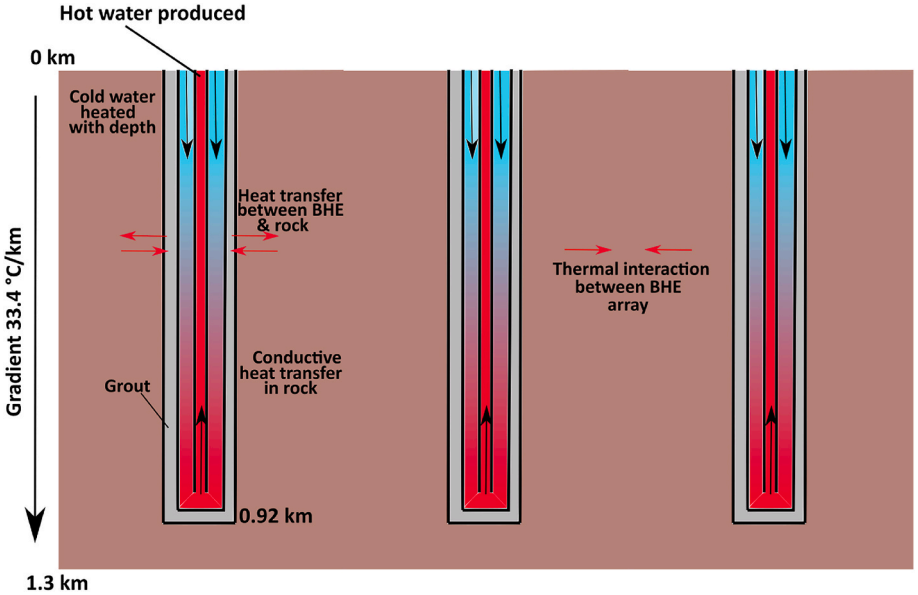

Fig. 2. Schematic of DBHE array and thermal interactions between components of the system.

conductive heat transfer in the surrounding rocks due to limited groundwater flow in shallow aquifers in the area [18] and previous studies have proven the influence of groundwater on DBHEs to typically be minimal [13].

A simple representation of the DBHE has been assumed here with a single grout layer and a single casing; a real setting typically has several casing and annular grout fills. There are four governing equations for heat transfer in (a) the rock formation, (b) the grout, (c) the borehole casing and (d) the central coaxial pipe. The governing equation in the rock formation is given by the energy balance ([13,42]):

$$\frac{\partial}{\partial t}\left[\varphi\rho_f c_f + (1-\varphi)\rho_r c_r\right]T_r - \nabla\cdot(\Lambda_r\cdot\nabla T_r) = H_r \quad [1]$$

where φ is the rock porosity, ρ_r is the rock bulk saturated density, ρ_f is the circulating fluid density, T_r is the rock temperature, c_r is the bulk saturated specific heat capacity of the rock and c_f is the specific heat capacity of the fluid. Porosity was set to zero as advective heat flux was not modelled in the surrounding rock. Properties were assumed to be constant without dependence on temperature and pressure. H_r is the source term and Λ_r is the thermal hydrodynamic dispersion tensor, which depends on the bulk thermal conductivity of the rock λ_r. Between the rock and the DBHE, a heat flux (q_{nT_r}) boundary condition is adopted:

$$q_{nT_r} = -(\Lambda_r\cdot\nabla T_r) \quad [2]$$

Heat transfer by conduction dominates within the grout:

$$(1-\varphi_g)\rho_g c_g\frac{\partial T_g}{\partial t} - \nabla\cdot\left[(1-\varphi_g)\lambda_g\cdot\nabla T_g\right] = H_g \quad [3]$$

where the subscript g represents the grout. In the borehole casing (i.e., inlet, subscript i) and central coaxial pipe (i.e., outlet, subscript o), heat transfer is governed by the following advective heat transfer equations respectively:

$$\rho_f c_f\frac{\partial T_i}{\partial t} + \rho_f c_f \boldsymbol{v}_i\cdot\nabla T_i - \nabla\cdot(\Lambda_f\cdot T_i) = H_i \quad [4]$$

$$\rho_f c_f\frac{\partial T_o}{\partial t} + \rho_f c_f \boldsymbol{v}_o\cdot\nabla T_o - \nabla\cdot(\Lambda_f\cdot T_o) = H_o \quad [5]$$

where $\boldsymbol{v}_i$ and $\boldsymbol{v}_o$ are the inlet and outlet fluid velocity vectors, respectively. Λ_f represents the hydrodynamic thermo-dispersion tensor which in this example can be simplified to equal the fluid thermal conductivity (λ_f).

The horizontal thermal resistance to heat flow within the DBHE is analysed analogously to a resistor network. First, there is a thermal resistance to heat flow between the rock and grout (R_{gr}), then thermal resistance between the grout and the borehole casing (R_{fig}). Lastly, R_{ff} is the thermal resistance between the borehole casing and the central coaxial pipe (see Fig. 2). The boundary conditions at these three interfaces are influenced by their respective thermal resistances. Using the outer surface area at the relevant interface, the thermal resistances are expressed as heat transfer coefficients (Φ) which appear in the boundary conditions for the grout, borehole casing, and central coaxial pipe. The boundary condition for equation [3] can be expressed as:

$$q_{nT_g} = -\Phi_{gr}(T_r - T_g) - \Phi_{fig}(T_i - T_g) \quad [6]$$

In a similar procedure, the boundary conditions for equations [4] and [5] are expressed respectively as:

$$q_{nT_i} = -\Phi_{fig}(T_r - T_i) - \Phi_{ff}(T_o - T_i) \quad [7]$$

$$q_{nT_o} = -\Phi_{ff}(T_i - T_o) \quad [8]$$

The heat transfer coefficients in equation [6–8] are a function of the borehole casing diameter (d_{casing}), the central coaxial pipe diameter ($d_{central}$), and the borehole diameter (D_b). The heat transfer coefficients are given by: $\Phi_{gr} = 1/R_{gr}\pi D_b$, $\Phi_{fig} = 1/R_{fig}\pi d_{casing}$, and $\Phi_{ff} = 1/R_{ff}\pi d_{central}$. See for example, [43], on how to compute the thermal resistances.

2.2. Evaluation of system efficiency

The boundary condition prescribed at the top of the DBHE as the thermal power (P_{DBHE}) was based on the inlet and outlet fluid temperature from the heat pump to the wellbore. Thus, each DBHE was treated independently, with its own 50 kW heat pump (in reality, boreholes in an array may alternatively be connected in parallel to a single large heat pump, such that they all experience the same T_{in} but varying thermal power extraction). The thermal power of the DBHE can be calculated as (e.g. Refs. [26,27]):

$$P_{DBHE} = \rho_f c_f Q(T_{out} - T_{in}) \quad [9]$$

where Q is the volumetric flow rate and other parameters are listed as above in section 2.1 (or Table 1). The thermal power was pre-set at 50 kW for each borehole and a temperature difference between the inlet and outlet imposed. The equivalent average building thermal load was then calculated as the output from the heat pump. The efficiency of the system can be calculated using the coefficient of performance (COP) which is the ratio of the thermal energy supplied to the building from the heat pump ($P_{building}$) and the electrical energy consumed by the heat pump (W_{hp}) (e.g., Ref. [36]).

$$COP = \frac{P_{building}}{W_{hp}} \quad [10]$$

The COP equation uses a simple linear relationship between the fluid leaving the heat pump and the outlet temperature of the DBHE. This assumes fluid in the heat pump is heated to a temperature of 35 °C

Table 1
Thermo-physical parameters of the model. Model parameters are either taken from literature, assumed unpublished values (assembled by Westaway [28] and Banks [29]), calculated values or given as the most likely value. Sources from literature include: Younger et al. [18], Kimbell et al. [30], Westaway and Younger [31], Brown et al. [8], Gebski et al. [32], Bott et al. [33], England et al. [34], Lesniak et al. [35]. Note the inner pipe is the coaxial pipe and the outer pipe is the casing. The real nature of the casing situation is notably more complex than that modelled. The thermal properties of the rock in the subsurface are taken as the weighted average from Kolo et al. [22].

Parameter	Value	Units	Symbol
Borehole Depth [18]	922	m	L
Borehole Diameter [18]	0.216	m	D_b
Outer Diameter of Inner Pipe	0.1005	m	–
Thickness of Inner Pipe	0.00688	m	–
Thickness of Outer Pipe	0.0081	m	–
Thickness of Grout	0.01905	m	–
Thermal Conductivity of Polyethylene Inner Pipe	0.45	W/(m.K)	–
Thermal Conductivity of Steel Outer Pipe	52.7	W/(m.K)	–
Density of Rock [22,30]	2480	kg/m^3	ρ_r
Thermal Conductivity of Rock	2.55	W/(m.K)	λ_r
Specific Heat Capacity of Rock [22,31,35]	950	J/(kg.K)	C_r
Volumetric heat capacity of rock	2.356	MJ/(m^3.K)	–
Density of Grout	995	kg/m^3	ρ_g
Thermal Conductivity of Grout	1.05	W/(m.K)	λ_g
Specific Heat Capacity of Grout	1200	J/kgK	C_g
Density of Fluid [8]	998	kg/m^3	ρ_f
Thermal Conductivity of Fluid	0.59	W/(m.K)	λ_f
Specific Heat Capacity of Fluid	4179	J/kgK	C_f
Heat Load Extracted	50	kW	P_{DBHE}
Surface Temperature [32]	9	°C	–
Geothermal Gradient [18,32]	33.4	°C/km	–
Volumetric Flow Rate	0.005	m^3/s	Q
Circulation Pump Efficiency	70	%	n

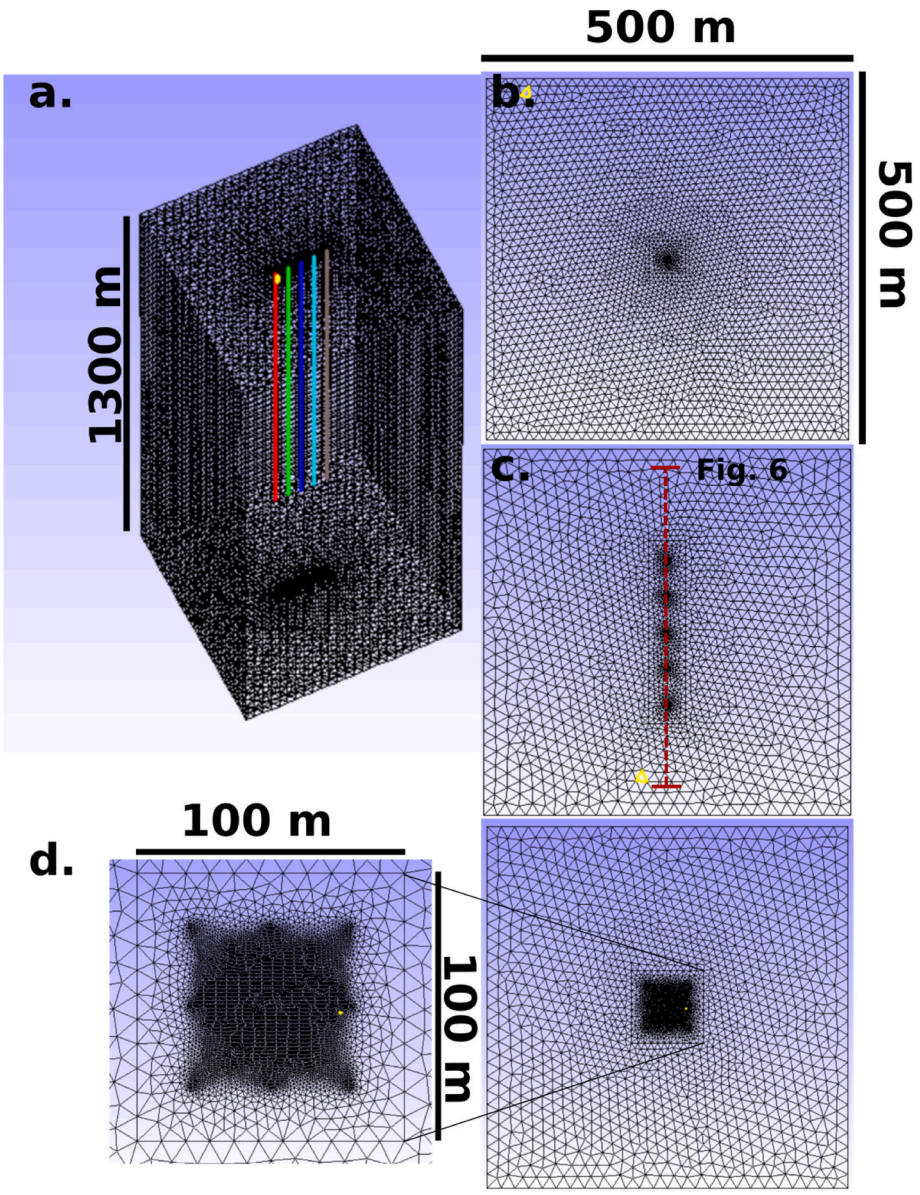

Fig. 3. (a) Example 3D mesh for a line array, (b) example 2D plan view of 1 DBHE, (c) example 2D plan view of a line array and (d) example 2D plan view of a 3 × 3 square array. Location of Fig. 6 cross slice highlighted.

before being used for spatial heating [37]:

$$COP = (T_{out} \times 0.083) + 3.925 \quad [11]$$

where T_{out} is in °C. This implies that, when the fluid entering the heat pump is 0 °C, the COP is 3.925. The thermal power for the DBHE is related to building heat load as:

$$P_{DBHE} = P_{building} - W_{hp} \quad [12]$$

Furthermore, a relationship between heat extracted from the DBHE and heat load of the building can be established as:

$$P_{building} = \frac{COP}{COP - 1} P_{DBHE} \quad [13]$$

When exploiting geothermal energy from a DBHE the power from the circulation pump (W_{cp}) should also be considered as pressure drop will require energy to circulate the fluid. As such, the coefficient of system performance (*CSP*) can be used to evaluate the total electrical energy used by the system to extract the heat [13]:

$$CSP = \frac{P_{building}}{W_{hp} + W_{cp}} \quad [14]$$

The energy used by the circulating pump was calculated as [27]:

$$W_{cp} = \frac{\Delta P \times Q}{n} \quad [15]$$

where ΔP is the pressure drop in the DBHE and n is the efficiency of the pump (assumed to be 70%). The pressure drop was calculated as the summation of pressure drop in the central pipe and annular space. Pressure drop was calculated for each component using the Darcy-Weisbach equation and Petukhov's version of the friction factor, valid down to Re = 3000 [13,38,39]:

$$\Delta p = \frac{L \rho_f V_f^2}{2 D_h [0.79 \ln(Re) - 1.64]^2} \quad [16]$$

where L is the length of the pipe, V_f is the mean velocity of the inlet, D_h is the hydraulic diameter, and Re is the Reynolds number (assumed to be

for turbulent flow in this study).

2.3. Model parameters, boundary and initial conditions

For the Newcastle Helix area, under initial conditions the model was set up to increase in temperature with depth, subject to a geothermal gradient of 33.4 °C/km with a surface temperature of 9 °C. The temperature of all DBHE components was initially assumed to be in equilibrium with the surrounding rock (i.e., $T_{grout} = T_{fluid} = T_{rock}$). The boundary conditions were defined as follows: (i) upper surface, Dirichlet boundary condition, with constant surface temperature at 9 °C, (ii) lower surface, Neumann boundary condition with constant basal heat flux of 85.17 mW m^{-2} to reflect the geothermal gradient and thermal conductivity (iii) lateral boundaries, Neumann no flow boundary conditions with heat flux set to zero. The lateral and bottom boundaries of the model were also set to a distance far enough from the DBHEs to minimise any interactions caused by domain boundaries. The minimum nodal domain was set to be 500 × 500 × 1300 m (x,y,z) and the depth of each DBHE to 920 m.

Model data has been collated from a series of sources (Table 1), with in-situ data used where possible or else taken from literature. The thermal parameters utilised were assumed to be the bulk saturated properties for the rock taken as a weighted average through the vertical dimension of the model [22]. To identify the smallest spacing required between DBHEs to reduce thermal interference, models were initially simulated for 20 years of constant heat load operation.

The smallest spacing was then identified as the point that any DBHEs fluid circulation temperature dropped below 0 °C, which is anticipated to cause freezing in the DBHE or heat pump as it is assumed fresh water was the circulating fluid. This is a low threshold and in reality risk of freezing could start at ~3/4 °C.

Long term simulations were then conducted to compare the influence of intermittent and constant heat load extraction over the lifetime of 20 years. In all cases a 50 kW heat load was imposed for each DBHE with a 5 l/s flow rate. A series of geometrical set ups were considered in the study (Fig. 3): a single DBHE, a 5 DBHE line array and a square 3 × 3 DBHE array. These were selected as notional cases that could be scaled to a maximum inter-borehole distance of 50 m within the area highlighted in Fig. 1. Spacing sizes of 20–50 m were modelled with incremental increases of 10 m.

2.4. Model benchmarking

The model was compared against an analytical solution by Beier [40] for the NSCDGB. A constant heat load of 50 kW was applied with circulation velocity of 5 l/s for a 20 year period (with parameters identical to that in Table 1); this is based on the single DBHE scenario outlined further in section 3.1. As highlighted in Fig. 4a and b, the models show good agreement with minimal discrepancy between inlet and outlet temperatures. Less than 0.12 °C difference was measured at the end of the simulation for the entire depth of the DBHE. Further benchmarking of OpenGeoSys against other solutions has also been conducted (e.g. Refs. [2,41]), providing high levels of confidence in the software for accurate simulations.

3. Results

3.1. Analysis of deep single borehole heat exchanger

Over the duration of the simulation, inlet and outlet temperatures decline with log time (Fig. 4a). The rapid temperature decrease in the first few days highlights thermal drawdown and cooling of the borehole (Fig. 4). As highlighted in Fig. 4a and c, prior to the cooling of the borehole, there is a warming over the length of the borehole and increase in the circulation fluid at the top of the borehole at ~10 h. This is caused by the extraction of the warm fluid at the base of the DBHE during the first cycle of circulation of fluid through the annular space and central pipe. Following this, the rock adjacent to the borehole cools rapidly (Fig. 4c).

The thermal field in proximity to the DBHE showed sharp concaving upwards with limited thermal cooling to within 60 m (measured to <0.1 °C) (Fig. 4d). At the end of the simulation the outlet and inlet

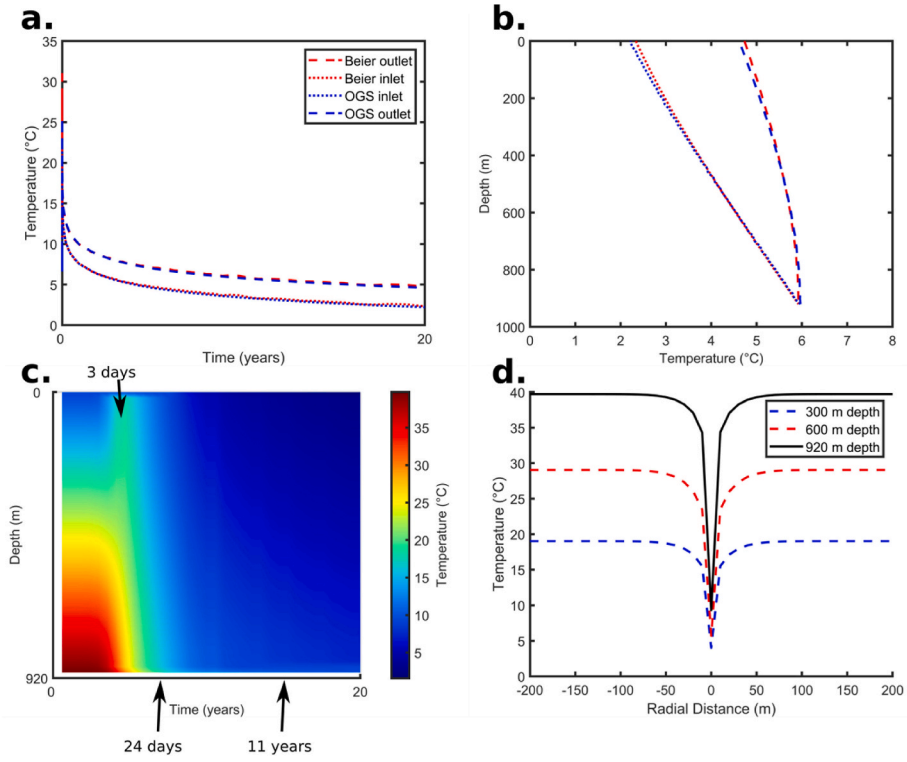

Fig. 4. Comparison between model data for the single DBHE scenario and the analytical solution by Beier [40]. Fluid inlet and outlet temperature v (a) time and (b) depth. The blue is OGS data and the red is the analytical solution. Dashed lines represent outlet temperatures and the dotted lines are inlet temperatures. (c) Thermal evolution of the rock adjacent to the DBHE with time (note time steps are not uniform and increase with time). (d)Temperature profiles in the rock around the DBHE (located at point 0) after 20 years of simulation.

temperature, within the central pipe and annular space, were 4.6 and 2.2 °C, respectively. The results from the initial single well simulation were utilised as a base case to compare with the DBHE arrays and the increased thermal cooling of a system caused by thermal interference between different boreholes. Furthermore, it is also evident that if a constant heat load is applied for a period of 20 years, a heat pump will be required. Throughout the simulation the coefficient of system performance varied between 4.1 and 5.6. The former associated to low outlet temperatures at the end of the simulation and the latter to high outlet temperatures within the first few hours. The building load supported was 65.11 kW, recorded at the end of the simulation.

3.2. Analysis of deep borehole heat exchanger line array

Both the 20 m and 30 m inter-borehole spacing resulted in negative inlet temperatures of individual DBHEs within the line array, and a negative average inlet temperature (Fig. 5a). This highlights the thermal cooling of the surrounding rock around each individual DBHE and thermal interference caused by the proximity of the spacing (Fig. 6).

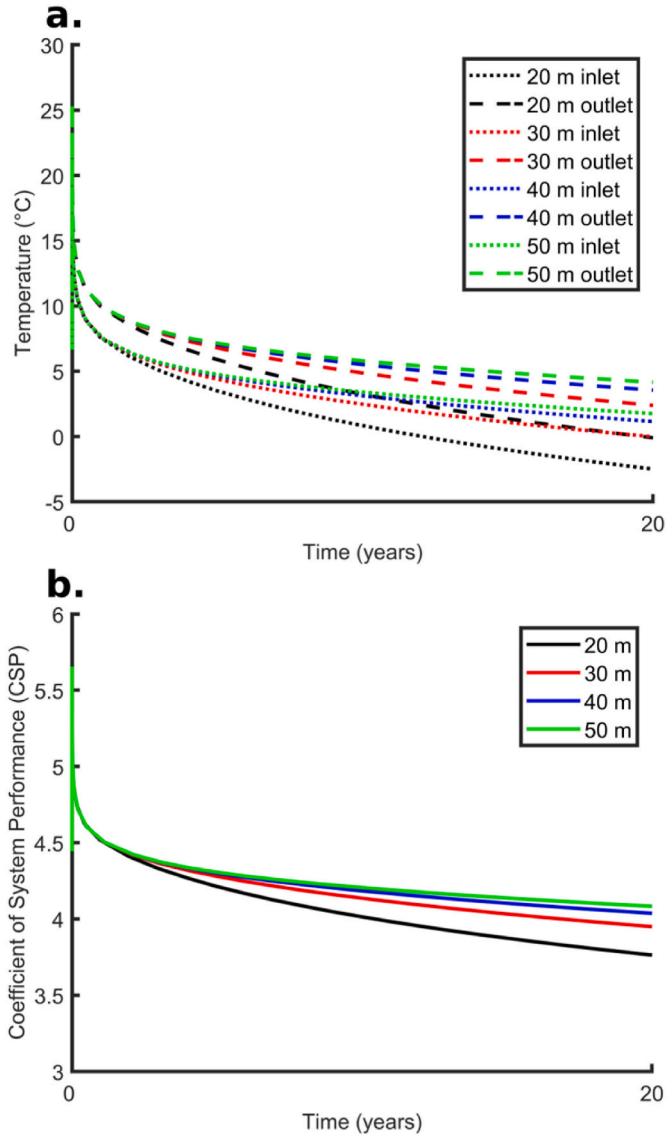

Fig. 5. (a) Average inlet and outlet temperatures across DBHEs for different inter-borehole spacing for line arrays. Inlet (annular space) is the dotted line and outlet (central pipe) is the dashed line. (b) Coefficient of system performance evolution versus time.

Both the 40 and 50 m inter-borehole spacing scenarios showed more cooling of the fluid within each DBHE in contrast to the single well scenario, however, for both, the circulating fluid always stayed above 0 °C. The distributions of temperature in the subsurface around each array also reveal significant thermal drawdown in the subsurface, with greater cooling around the central DBHEs, particularly when inter-borehole spacing was 20 or 30 m. In Fig. 6a and b, the rock temperature at the point of the central DBHEs is approaching zero, or exceeding this for the 20 m spacing scenario. In Fig. 6c and d, the rock proximal to the DBHEs is always above zero with limited differences between the DBHEs within the array, which was interpreted as a result of restricted thermal interference.

Fig. 7a compares the maximum difference in circulation temperatures within the DBHE array. The difference was taken between the circulation fluid at the top of the inner and outermost borehole, with the difference between inlet and outlet temperatures equal due to the prescribed heat load for each DBHE. Results show that the innermost DBHE is significantly cooled in comparison to the outer DBHEs and further supports thermal cooling is greater at the centre of the array. Reduced inter-borehole spacing increases the maximum difference in circulation temperature. This was observed by the difference in maximum temperature between the 20 and 50 m spacing scenarios at year 20, where for the former a difference of 2.91 °C was observed and the latter 0.48 °C.

Based off the average outlet/inlet temperatures for each array (Fig. 5a) and the temperature profiles through the surrounding rock mass (Fig. 6), it appears a minimum spacing of 40 m between DBHEs is required (if 0 °C is the cut-off temperature). In reality, greater inter-borehole spacing will be better for minimising thermal interference. Furthermore, when considering the efficiency of the system the CSP is reduced for the 20 and 30 m scenarios (Fig. 5b), indicating more energy is required to operate the heat pump, caused by the lower outlet temperatures. Whilst a heat load of 50 kW was imposed per DBHE the building heat load supported on average per DBHE at the end of the simulation ranged from 67 to 65 kW (for 20–50 m, respectively).

3.3. Analysis of deep borehole heat exchanger square array

Similarly to line arrays, the 20–30 m inter-borehole spacing resulted in fluid temperatures reducing below 0 °C by the end of operation (Fig. 8a). In contrast, however, the 40 m spacing also showed a drop in average borehole fluid inlet temperature below 0 °C before the end of the simulation. This highlights the geometry of the array results in more thermal interference between boreholes. The cooling of the system is also reflected when considering the system efficiency. At the end of the simulation the coefficient of system performance is lower for each spacing increment in comparison to that of the line array and single DBHE. At 20 years, the minimum and maximum CSP is 3.29 and 4.04, respectively for the 20 and 50 m spacing. More energy is required by the heat pump per DBHE too, due to decreased outlet temperatures with a similar building heat load per DBHE given as 70–66 kW, respectively.

The maximum difference in temperature between inner and outer boreholes was greater than that for line arrays. Fig. 7b highlights that there is a difference in excess of 6 °C at the end of the 20 year simulation. Significant cooling occurs in the central DBHE. This is due to more DBHEs within a smaller area mining more heat from the ground, limiting the thermal replenishment. The warmest DBHE in each of the arrays was located in each corner.

3.4. Impact of operation on longevity

To test if the results on spacing and array geometry were dependent on operation of the system, the performance of different arrays under both constant heat load extraction and intermittent heat extraction with periods of recovery were compared. In reality operational cycles will have short-to-long term extraction patterns; however, in this study they

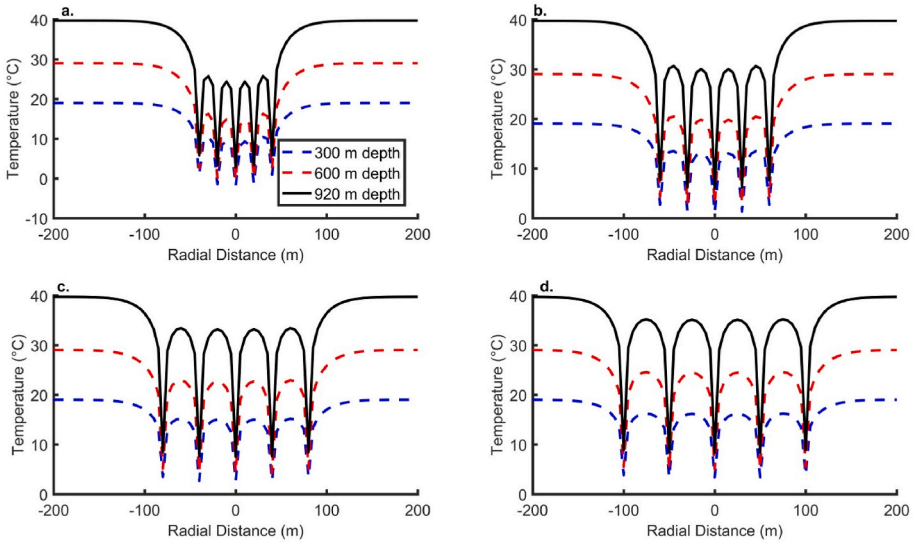

Fig. 6. Temperature profiles through the ground for different array sizes, (a) 20 m spacing, (b) 30 m spacing, (c) 40 m spacing, (d) 50 m spacing. Profiles taken from north to south through the array (i.e., top to bottom on Fig. 3c as indicated).

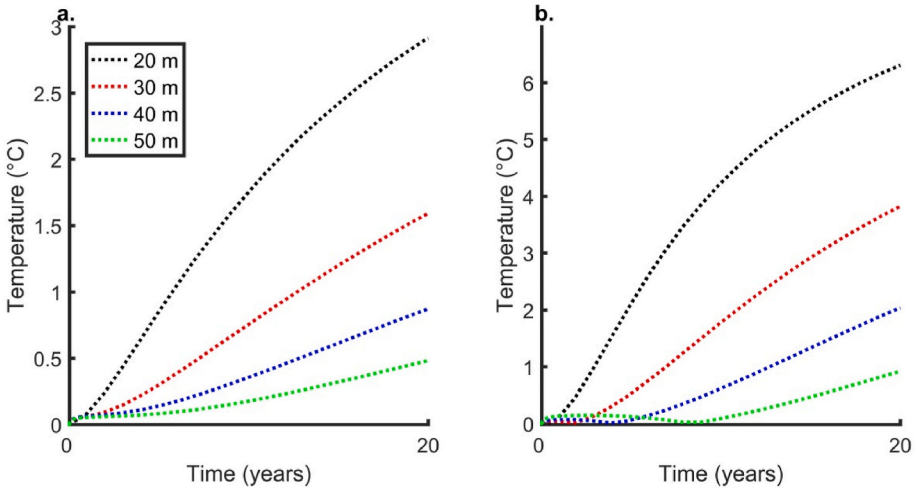

Fig. 7. Maximum difference in inlet temperatures between different DBHEs within the array, (a) is for line arrays and (b) for square arrays. Note the maximum difference in inlet temperatures is equal to that of outlet temperatures.

were investigated using the average heat load applied to a typical heating season in the UK (6 months), followed by an equal amount of recovery in the subsurface. The different arrays were then tested and compared to see if the method of operation could enable smaller inter-borehole spacing dependent on the mode of operation and geometry.

Mode of operation significantly impacted the temperature of the circulation fluid within the DBHEs. For all arrays constant heat load operation resulted in a greater temperature drop in comparison to intermittent operation. Periods of recovery allow warming of the DBHEs and replenishment of the resource. For example, consider the inter-borehole spacing for both line and square arrays where the circulation temperature dropped below 0 °C for constant heat load extraction (i.e., 30 m for the line array and 40 m for the square array). Both the line and square arrays previously dropped to temperatures unlikely to be operable for long term extraction using a constant heat load. When implementing an intermittent source term they showed reduced cooling in the subsurface and within the DBHE for the lifetime of operation (Fig. 9). At the end of the last extraction period under intermittent operation (at 19.5 years) the inlet temperature was 5.7, 4.7 and 4.6 °C for the single DBHE, line and square arrays respectively (Table 2). The minimum temperatures of the fluid at surface level were therefore, far higher than during constant heat load operation. When identifying the minimum spacing under intermittent operation for both array geometries the 10 m (line) and 20 m (square) spacing showed circulation temperatures in the extraction period to drop below 0 °C. Therefore, the minimum spacing for line and square arrays was 20 and 30 m, respectively.

Furthermore, the amount of energy extracted during intermittent operation over the lifetime of the system in comparison to the constant heat load operation was considered. When using the same constant heat rate less energy will be extracted during intermittent operation. Therefore, further testing was undertaken such that the total energy extracted during the lifetime was equal for both modes of operation.

For the single DBHE example, the constant heat load operation amount was reduced to an extraction rate of 25 kW to match the 50 kW intermittent operation total thermal energy extraction. Difference in circulation temperatures are highlighted in Fig. 10. The figure shows that the total thermal energy extracted over the year is as important as the mode of operation. When the total heat extracted is equal for constant heat load and intermittent modes, the smaller heat extraction rate imposed for constant heat load results in far less cooling of the DBHE

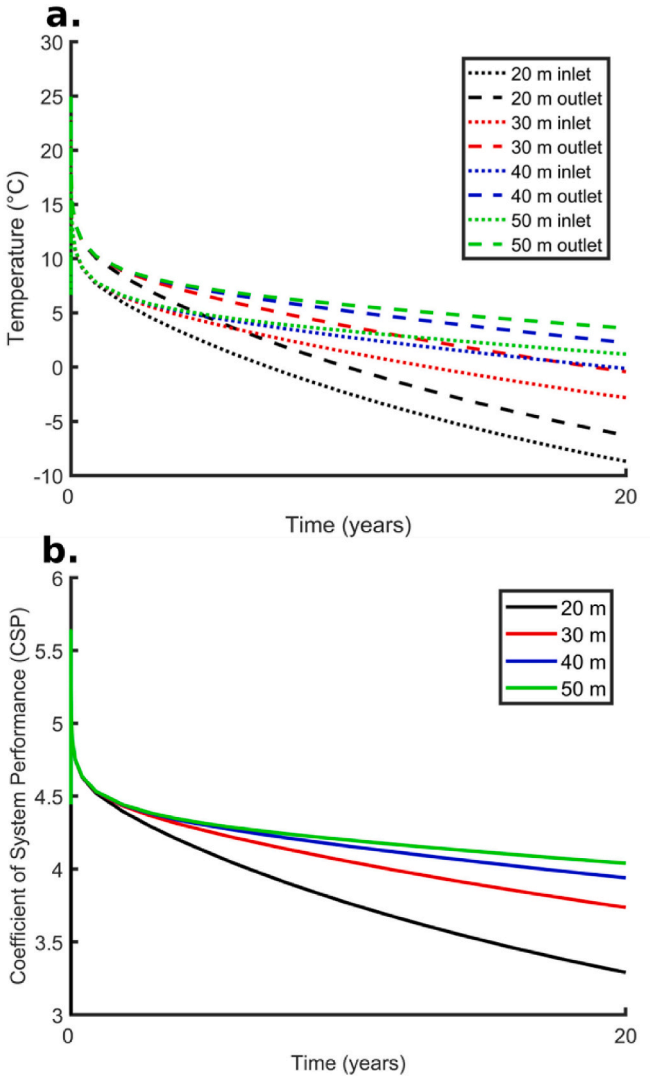

Fig. 8. (a) Average inlet and outlet temperatures across DBHEs for different inter-borehole spacing for square arrays. Inlet (annular space) is the dotted line and outlet (central pipe) is the dashed line. (b) Coefficient of system performance evolution versus time.

fluid. This results in higher outlet temperatures and improved CSP. Therefore, there are benefits in applying a constant heat load over the period of operation, however, practically this may not correspond to periods of high demand and the heat extracted is more likely to contribute to demand, rather than meet it directly.

4. Discussion: implications of modes of operation, geometry and borehole spacing on array performance

When considering constant heat load operation over the lifetime of a DBHE array, this study has shown line arrays may be more suited for operation of DBHE arrays. From a technical perspective they require reduced inter-borehole spacing and also have the benefit of taking up less surface space. In contrast, square arrays demonstrate poorer performance and increased thermal interference between each DBHE. Other studies have suggested a low minimum inter-borehole spacing (15 m) than established in this study [16,17]; however, these studies model intermittent operation only. When comparing intermittent operation (6 months extraction v 6 month recovery) with constant heat load operation it appears a reduced inter-borehole spacing can be applied. For the single DBHE, 30 m line array and 40 m square array the intermittent operation mode resulted in far higher minimum inlet and outlet temperatures in comparison to the constant heat load extraction rate. Intermittent operation allows replenishment of the heat extracted and reduced thermal drawdown, implying far smaller inter-borehole spacing can be supported. Although, when investigating the total energy extracted (i.e., constant heat load of 25 kW and intermittent at 50 kW) it appears the 25 kW constant heat load operation will improve thermal performance and system efficiency.

This study also has local connotations to the Newcastle Helix area where the array could theoretically be deployed. The large spacing required for both types of arrays means the spatial area required on the surface must be carefully considered before development. Prior to scaling of DBHE geothermal projects, this study has highlighted the method of operation is important to consider, with intermittent operation allowing more boreholes to be situated within the area. Furthermore, future developments may also consider the impact of incorporating a splitter if utilising the thermal energy in a heat network. When adopting a multi-DBHE system it appears theoretically the heat load of the adjacent Urban Sciences Building can be supported for the duration of the year. Zirak et al. [23] modelled the heat demand to be between 989 MWh and 792 MWh per annum, with a significant decline in demand between May and October. Therefore, assuming most of this demand occurs in 6 months one borehole operating intermittently for 6 months extraction with at a rate of 50 kW could produce 219 MWh, which would supply the building ~285 MWh of heat (over 182.5 days).

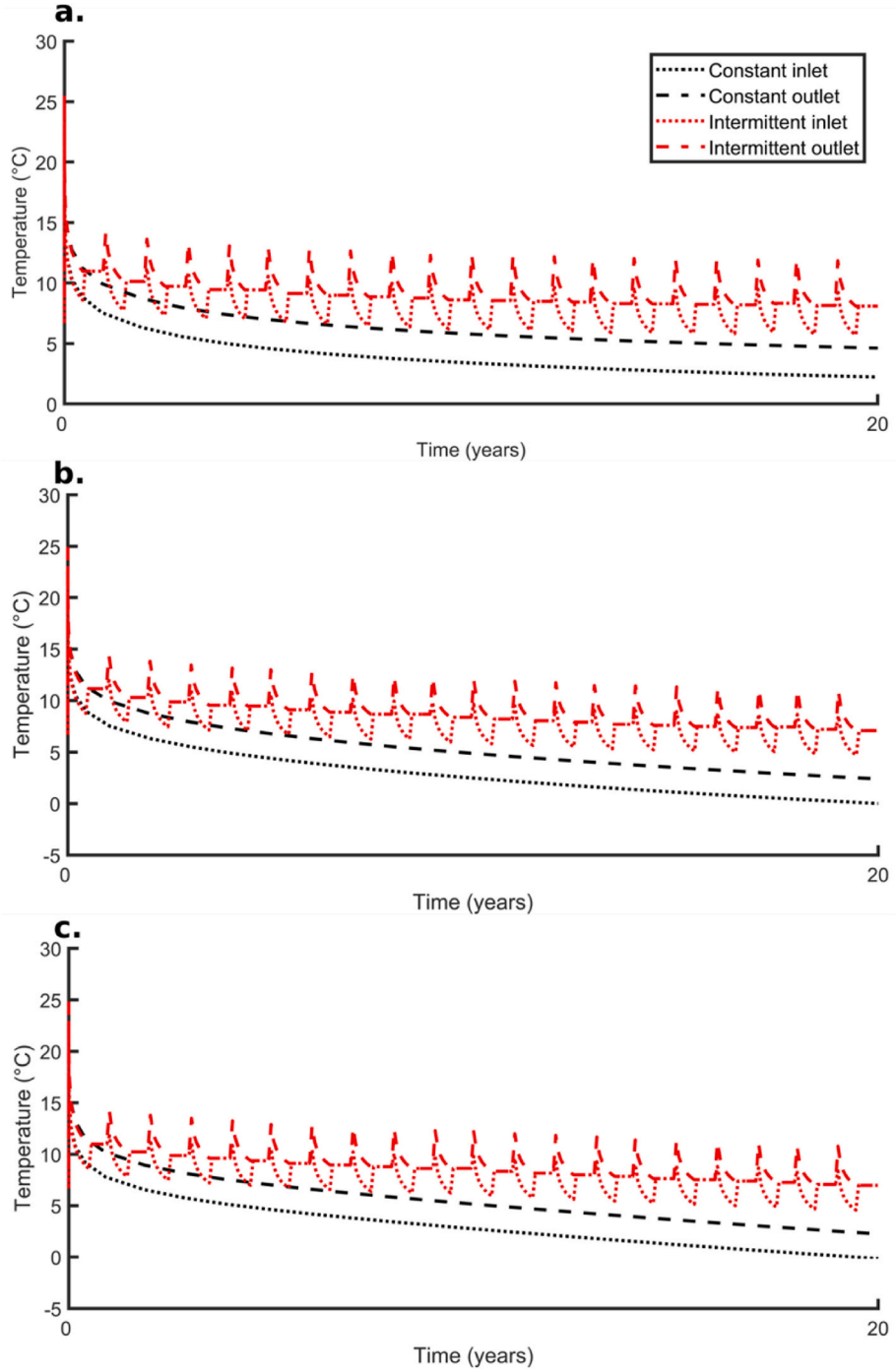

Fig. 9. Average inlet and outlet temperatures across DBHEs for different arrays (a) single DBHE, (b) line array with 30 m spacing and (c) square arrays with 40 m spacing. Inlet (annular space) is the dotted line and outlet (central pipe) is the dashed line. The fluid is assumed to stop circulating in the non-operational periods; thus the inlet and outlet temperatures are approximately static but trend towards surface temperature. On commencement of operation, a small recovery is seen due to re-equilibration of deeper rock and fluid temperatures.

Table 2
Temperature at the end of the heating season (at year 19.5 for intermittent operation and 20 for constant).

	Intermittent Operation (°C)		Constant Heat Load Operation (°C)	
	Inlet	Outlet	Inlet	Outlet
Single DBHE	5.7	8.1	2.2	4.6
Line Array (30 m)	4.7	7.1	−0.0	2.4
Square Array (40 m)	4.6	7	−0.1	2.3

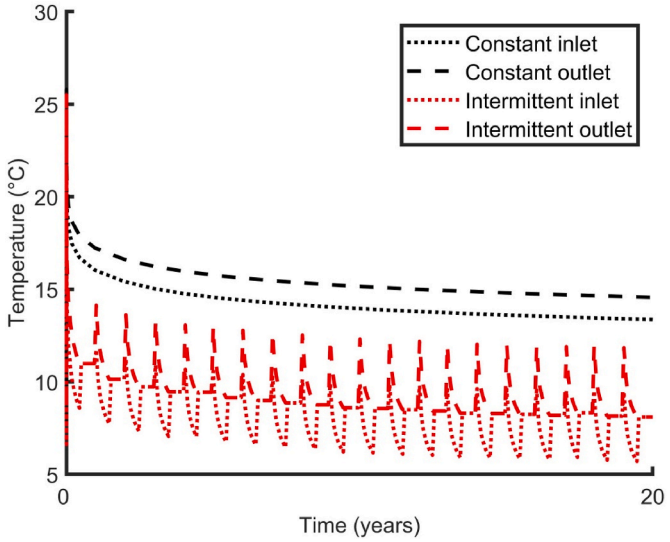

Fig. 10. Average inlet and outlet temperatures for a single DBHE with constant heat load of 25 kW (black) and an intermittent mode of operation of 50 kW for 6 months (red). Inlet (annular space) is the dotted line and outlet (central pipe) is the dashed line. In both cases, a total of 219 MWh/a heat is extracted. The fluid is assumed to stop circulating in the non-operational periods; thus the inlet and outlet temperatures are approximately static but trend towards surface temperature. On commencement of operation, a small recovery is seen due to re-equilibration of deeper rock and fluid temperatures.

If looking to meet all the demand using a DBHE line array approximately 4 DBHEs would be required with a minimum spacing of 20 m. Further testing and optimisation would be required to match data in reality.

5. Conclusions

In this study, a numerical model was established with the aim of investigating scalability of DBHEs in the form of operation as an array. Long term performance of different array geometry and spacing was tested, with further focus on the impact of operation. The key conclusions were:

- Initial benchmarking in comparison to the analytical solution by Beier [40] show OpenGeoSys software to have a high level of accuracy, with minimal discrepancy (<0.12 °C) in comparison.
- When operating using a constant heat load of 50 kW for 20 years the minimum inter-borehole spacing requirement for line arrays was 40 m and for square arrays 50 m.
- When operating using intermittent heat load of 50 kW for 20 years the minimum inter-borehole spacing requirement for line arrays was 20 m and for square arrays 30 m.
- Smaller heat loads are likely to require a reduced minimum spacing for both modes of operation. Lower fluid circulation temperatures (i.e., circulating fluid with anti-freeze) will also allow the use of borehole spacing less than the proposed “minima".
- The coefficient of system performance shows high degradation when the average outlet temperature of the array drops below zero, with CSP ranging from 5.6 to 3.29 throughout the study.
- For the NSCDGB the line arrays modelled have greater CSPs and require less space between DBHEs as they allow for less thermal interference in contrast to a square array.
- Intermittent operation results in reduced inter-borehole spacing and is likely to allow increased heat extraction rates to be implemented on the array with increased recovery periods.
- When considering the total heat extracted, performance is best when a constant heat load is applied, rather than higher heat loads over shorter time periods. This minimises thermal drawdown in the system and increases the efficiency.

CRediT authorship contribution statement

Christopher S. Brown: Conceptualization, Methodology, Software, Data curation, Formal analysis, Writing – original draft, preparation, Writing – review & editing. **Isa Kolo:** Methodology, Software, Writing – original draft, preparation, Writing – review & editing. **Gioia Falcone:** Writing – review & editing, Supervision. **David Banks:** Writing – review & editing, Supervision.

Declaration of competing interest

The authors declare that they have no known competing financial interests or personal relationships that could have appeared to influence the work reported in this paper.

Acknowledgments

We would like to show appreciation to the UKRI EPSRC (grant reference numbers EPSRC EP/T022825/1 and EPSRC EP/T023112/1) for funding this research. The funding sources are for the NetZero GeoRDIE (Net Zero Geothermal Research for District Infrastructure Engineering) and INTEGRATE (Integrating seasoNal Thermal storagE with multiple enerGy souRces to decArobonise Thermal Energy) projects, respectively. For the purpose of open access, the author has applied a Creative Commons Attribution (CC BY) licence to any Author Accepted Manuscript version arising from this submission.

References

[1] A. Galgaro, Z. Farina, G. Emmi, M. De Carli, Feasibility analysis of a Borehole Heat Exchanger (BHE) array to be installed in high geothermal flux area: the case of the Euganean Thermal Basin, Italy, Renew. Energy 78 (2015) 93–104.
[2] J. Randow, S. Chen, K. Lubashevsky, S. Thiel, T. Reinhardt, K. Rink, R. Grimm, A. Bucher, O. Kolditz, H. Shao, Modeling neighborhood-scale shallow geothermal energy utilization: a case study in Berlin, Geoth. Energy 10 (1) (2022) 1–26.
[3] R. Wang, F. Wang, Y. Xue, J. Jiang, Y. Zhang, W. Cai, C. Chen, Numerical study on the long-term performance and load imbalance ratio for medium-shallow borehole heat exchanger system, Energies 15 (9) (2022) 3444.
[4] DECC, Energy bill 2015-2016. Infrastructure Act. Department of energy and climate change. https://assets.publishing.service.gov.uk/government/uploads/system/uploads/attachment_data/file/490997/Infrastructure_Act_2015_Energy_Bill_2015-16_Keeling_Schedule_.pdf, 2016. (Accessed 30 September 2022).
[5] C. Alimonti, D. Berardi, D. Bocchetti, E. Soldo, Coupling of energy conversion systems and wellbore heat exchanger in a depleted oil well, Geoth. Energy 4 (1) (2016) 1–17.
[6] G. Falcone, X. Liu, R.R. Okech, F. Seyidov, C. Teodoriu, Assessment of deep geothermal energy exploitation methods: the need for novel single-well solutions, Energy 160 (2018) 54–63, https://doi.org/10.1016/j.energy.2018.06.144.
[7] T. Renaud, P.G. Verdin, G. Falcone, Conjugated numerical approach for modelling DBHE in high geothermal gradient environments, Energies 13 (22) (2020) 6107, https://doi.org/10.3390/en13226107.
[8] C.S. Brown, N.J. Cassidy, S.S. Egan, D. Griffiths, Numerical modelling of deep coaxial borehole heat exchangers in the Cheshire Basin, UK, Comput. Geosci. 152 (2021), 104752.
[9] H.R. Doran, T. Renaud, G. Falcone, L. Pan, P.G. Verdin, Modelling an unconventional closed-loop deep borehole heat exchanger (DBHE): sensitivity analysis on the Newberry volcanic setting, Geoth. Energy 9 (1) (2021) 1–24.
[10] L. Fang, N. Diao, Z. Shao, K. Zhu, Z. Fang, A computationally efficient numerical model for heat transfer simulation of deep borehole heat exchangers, Energy Build. 167 (2018) 79–88.
[11] J. Wołoszyn, Global sensitivity analysis of borehole thermal energy storage efficiency on the heat exchanger arrangement, Energy Convers. Manag. 166 (2018) 106–119.
[12] J. Wołoszyn, Global sensitivity analysis of borehole thermal energy storage efficiency for seventeen material, design and operating parameters, Renew. Energy 157 (2020) 545–559.
[13] C. Chen, H. Shao, D. Naumov, Y. Kong, K. Tu, O. Kolditz, Numerical investigation on the performance, sustainability, and efficiency of the deep borehole heat exchanger system for building heating, Geoth. Energy 7 (1) (2019) 18, https://doi.org/10.1186/s40517-019-0133-8.
[14] H. Skarphagen, D. Banks, B.S. Frengstad, H. Gether, Design considerations for borehole thermal energy storage (BTES): a review with emphasis on convective heat transfer, Geofluids 2019 (2019).

[15] X. Hu, J. Banks, L. Wu, W.V. Liu, Numerical modeling of a coaxial borehole heat exchanger to exploit geothermal energy from abandoned petroleum wells in Hinton, Alberta, Renew. Energy 148 (2020) 1110–1123.
[16] W. Cai, F. Wang, S. Chen, C. Chen, J. Liu, J. Deng, O. Kolditz, H. Shao, Analysis of heat extraction performance and long-term sustainability for multiple deep borehole heat exchanger array: a project-based study, Appl. Energy 289 (2021), 116590.
[17] W. Cai, F. Wang, C. Chen, S. Chen, J. Liu, Z. Ren, H. Shao, Long-term performance evaluation for deep borehole heat exchanger array under different soil thermal properties and system layouts, Energy 241 (2022), 122937.
[18] P.L. Younger, D.A. Manning, D. Millward, J.P. Busby, C.R. Jones, J.G. Gluyas, Geothermal exploration in the fell sandstone formation (mississippian) beneath the city centre of Newcastle upon tyne, UK: the Newcastle science central deep geothermal borehole, Q. J. Eng. Geol. Hydrogeol. 49 (4) (2016) 350–363.
[19] L. Howell, C.S. Brown, S.S. Egan, Deep geothermal energy in northern England: insights from 3D finite difference temperature modelling, Comput. Geosci. 147 (2021), 104661.
[20] C.S. Brown, Regional geothermal resource assessment of hot dry rocks in Northern England using 3D geological and thermal models, Geothermics 105 (2022), 102503.
[21] GOW, Grants on the web. EPSRC EP/T022825/1. https://gow.epsrc.ukri.org/NGBOViewGrant.aspx?GrantRef=EP/T022825/1, 2020. (Accessed 11 April 2022).
[22] I. Kolo, C.S. Brown, G. Falcone, D. Banks, Closed-loop deep borehole heat exchanger: Newcastle science central deep geothermal borehole, in: European Geothermal Congress, 2022.
[23] M. Zirak, M. Royapoor, T. Gilbert, Cross-platform energy modeling for scalable urban energy simulation: a case-study, in: International Conference on Innovative Applied Energy (IAPE 2019), Newcastle University, 2019.
[24] Google Maps, [Google Maps location of Newcastle Helix area]. https://www.google.co.uk/maps/place/St.+James'+Park/@54.973498,-1.6274954,332m/data=!3m1!1e3!4m5!3m4!1s0x487e7734dc20d87b:0x2e911404fa537b88!8m2!3d54.975556!4d-1.621667, 2022. (Accessed 14 June 2022).
[25] I. Perser, I.A. Frigaard, A comprehensive study on intermittent operation of horizontal deep borehole heat exchangers, Energies 15 (1) (2022) 307.
[26] L. Dijkshoorn, S. Speer, R. Pechnig, Measurements and design calculations for a deep coaxial borehole heat exchanger in Aachen, Germany, International Journal of Geophysics 2013 (2013), https://doi.org/10.1155/2013/916541.
[27] J. Liu, F. Wang, W. Cai, Z. Wang, Q. Wei, J. Deng, Numerical study on the effects of design parameters on the heat transfer performance of coaxial deep borehole heat exchanger, Int. J. Energy Res. (2019) 1–16, https://doi.org/10.1002/er.435716LIUETAL.
[28] R. Westaway, Rock Thermal Properties for Newcastle Helix Site, Internal University of Glasgow report for NetZero GeoRDIE project, 2020 (unpublished).
[29] D. Banks, Thermal Properties of Well Construction Materials - Newcastle Science Central Borehole, Internal University of Glasgow report for NetZero GeoRDIE project, 2021 (unpublished).
[30] G.S. Kimbell, R.M. Carruthers, A.S.D. Walker, J.P. Williamson, Regional Geophysics of Southern Scotland and Northern England. Version 1.0 on CD-ROM, British Geological Survey, Keyworth, 2006. Available from, https://shop.bgs.ac.uk/Bookshop/product.cfm?p_id=KRGSCD.
[31] R. Westaway, P.L. Younger, Unravelling the relative contributions of climate change and ground disturbance to subsurface temperature perturbations: case studies from Tyneside, UK, Geothermics 64 (2016) 490–515.
[32] J.S. Gebski, J. Wheildon, A. Thomas-Betts, Investigations of the UK Heat Flow Field (1984-1987), British Geological Survey, Nottingham, 1987, p. 60. Report WJ/GE/87/6.
[33] M.H.P. Bott, G.A.L. Johnson, J. Mansfield, J. Wheilden, Terrestrial heat flow in north-east England, Geophys. J. Roy. Astron. Soc. 27 (1972) 277–288.
[34] P.C. England, E.R. Oxburgh, S.W. Richardson, Heat refraction and heat production in and around granite plutons in north–east England, Geophys. J. Int. 62 (1980) 439–455.
[35] B. Lesniak, Ł. Słupik, G. Jakubina, The determination of the specific heat capacity of coal based on literature data, Chem 67 (2013) 560–571.
[36] S.K. Kim, G.O. Bae, K.K. Lee, Y. Song, Field-scale evaluation of the design of borehole heat exchangers for the use of shallow geothermal energy, Energy 35 (2) (2010) 491–500, https://doi.org/10.1016/j.energy.2009.10.003.
[37] P. Hein, O. Kolditz, U.-J. Görke, A. Bucher, H. Shao, A numerical study on the sustainability and efficiency of borehole heat exchanger coupled ground source heat pump systems, Appl. Therm. Eng. 100 (2016) 421–433, https://doi.org/10.1016/j.applthermaleng.2016.02.039.
[38] B.S. Petukhov, Heat transfer and friction in turbulent pipe flow with variable physical properties, in: J.P. Hartnett, T.F. Irvine (Eds.), Advances in Heat Transfer, ume 6, Elsevier, 1970, pp. 503–564, https://doi.org/10.1016/S0065-2717(08)70153-9.
[39] F.P. Incropera, D.P. DeWitt, T.L. Bergmann, A.S. Lavine, Fundamentals of Heat and Mass Transfer, sixth ed., John Wiley and Sons, 2007.
[40] R.A. Beier, Thermal response tests on deep borehole heat exchangers with geothermal gradient, Appl. Therm. Eng. 178 (2020), 115447.
[41] W. Cai, F. Wang, J. Jiang, Z. Wang, J. Liu, C. Chen, Long-term performance evaluation and economic analysis for deep borehole heat exchanger heating system in Weihe basin. Front, Earth Sci. 10 (2022), 806416.
[42] H. Shao, P. Hein, A. Sachse, O. Kolditz. *Geoenergy modeling II: shallow geothermal systems*, Springer International Publishing, 2016.
[43] H.J. Diersch, D. Bauer, W. Heidemann, W. Rühaak, P. Schätzl, Finite element modeling of borehole heat exchanger systems: Part 1. Fundamentals, Comput. Geosci. 37 (8) (2011) 1122–1135.